

# Quantum chaos in open systems: a quantum state diffusion analysis

Todd A. Brun, Ian C. Percival, and Rüdiger Schack  
Department of Physics  
Queen Mary and Westfield College, University of London  
Mile End Road, London E1 4NS, England

November 20, 2018

PACS 03.65.-w, 05.45.+b, 03.65.Db, 03.65.Sq

## Abstract

Except for the universe, all quantum systems are open, and according to quantum state diffusion theory, many systems localize to wave packets in the neighborhood of phase space points. This is due to decoherence from the interaction with the environment, and makes the quasiclassical limit of such systems both more realistic and simpler in many respects than the more familiar quasiclassical limit for closed systems. A linearized version of this theory leads to the correct classical dynamics in the macroscopic limit, even for nonlinear and chaotic systems. We apply the theory to the forced, damped Duffing oscillator, comparing the numerical results of the full and linearized equations, and argue that this can be used to make explicit calculations in the decoherent histories formalism of quantum mechanics.

QMW Theory Preprint QMW-PH-95-33

# 1 Introduction

One of the chief questions in quantum theory is how classical behavior arises in quantum mechanical systems. A naïve description of a closed system, using the Schrödinger equation, very quickly loses all resemblance to classical mechanics. Even a highly localized wave packet can, given sufficient time, spread until it occupies all accessible regions of phase space. Such delocalized states are highly non-classical, and quite unlike what we normally observe.

However, if there is any significant interaction with the environment, such as a measurement, the system becomes open, and the Schrödinger equation is no longer valid. Macroscopic systems, with the exception of the entire universe, are never completely isolated. Even in interstellar space, interactions with thermal background radiation and encounters with stray atoms prevent macroscopic superpositions from arising [1].

The master equation approach has long been used to treat open quantum systems. In it, one averages over the unknown effects of interaction with the environment to compute the probabilities of possible output states. This has been used in an enormous range of experimental set-ups.

Modern experiments, however, often enable one to follow the behavior of a single quantum system as it evolves, influenced (but not destroyed) by the environment, including the measurement apparatus itself. Quantum state diffusion (QSD) provides a formalism which can be used to describe such situations [2]. In it, a system is always in a pure state, evolving according to a stochastic nonlinear Langevin-Itô equation. The equation includes both collective effects of the environment (such as dissipation and localization) and random fluctuations. For most open systems, the classical limit is qualitatively very different than for closed systems. QSD shows this particularly clearly, with its dynamical localization producing wave packets which follow approximately classical trajectories. In this sense, the classical limit of open systems is far simpler than that for closed systems.

In section 2 we describe the QSD formalism, and compare it with the decoherent histories approach to quantum mechanics [3, 4, 5, 6, 7, 8]. It has

recently been shown that these two approaches are related, and in fact provide complementary views of systems interacting with environments [9].

In section 3 we examine the quantum dynamics of linear systems and their classical limit, and how nonlinear systems can also be treated in this limit. We show that this is very different for open systems with localization than for closed systems. We briefly outline the importance of localization in efficient numerical simulation of QSD, and how it gives QSD remarkable advantages over other simulation methods for open systems. This builds on the results in [10], for a particular example.

In section 4 we examine the problem of quantum dissipative chaos. While considerable work has been done on quantum equivalents to classical Hamiltonian chaotic systems, very little has been done for dissipative chaos. In part, this is due to the challenging problems involved in studying dissipation in quantum systems. Spiller and Ralph [11] have shown how quantum state diffusion can be used to model dissipative chaotic systems. We examine a particular model, the forced, damped Duffing oscillator, to illustrate both the classical and quantum characteristics of dissipative chaos, and argue the relevance of these results to treatments using decoherent histories. The theoretical arguments are backed up by numerical results.

Finally, in section 5 we re-examine our results, and draw conclusions on the usefulness of QSD both as a theoretical and a practical tool in studying the quasiclassical limit of open quantum systems.

## 2 Quantum dynamics

### 2.1 Quantum state diffusion (QSD)

The master equation is used in the Markov approximation. It can then be expressed in *Lindblad form* [12]:

$$\dot{\rho} = -\frac{i}{\hbar}[\hat{H}, \rho] + \sum_{j=1}^m \left( \hat{L}_j \rho \hat{L}_j^\dagger - \frac{1}{2} \hat{L}_j^\dagger \hat{L}_j \rho - \frac{1}{2} \rho \hat{L}_j^\dagger \hat{L}_j \right), \quad (1)$$

where  $\rho$  is the density operator,  $\hat{H}$  is the Hamiltonian and the  $m$  operators  $\hat{L}_j$  are the *Lindblad operators*, which model the effects of the environment. Different choices of these  $\hat{L}_j$  have been used to simulate a wide range of physical situations, including measurements.

The evolution of a single open system is unpredictable. While an *ensemble* of systems may evolve in a perfectly deterministic manner, any *single* experimental run must have a strong stochastic component. There are many ways of “unraveling” the master equation into trajectories; the quantum state diffusion (QSD) formalism is one of these, with unique symmetry and localization properties [2, 13].

In QSD, a state evolves according to the Itô equation

$$\begin{aligned}
 |d\psi\rangle = & -\frac{i}{\hbar}\hat{H}|\psi\rangle dt + \sum_{j=1}^m \left( \langle \hat{L}_j^\dagger \rangle \hat{L}_j - \frac{1}{2} \langle \hat{L}_j^\dagger \rangle \langle \hat{L}_j \rangle - \frac{1}{2} \hat{L}_j^\dagger \hat{L}_j \right) |\psi\rangle dt \\
 & + \sum_{j=1}^m (\hat{L}_j - \langle \hat{L}_j \rangle) |\psi\rangle d\xi_j, \tag{2}
 \end{aligned}$$

where the  $d\xi_j$  are  $m$  independent complex random differential variables representing a complex Wiener process. They obey relationships

$$M(d\xi_i) = M(d\xi_i d\xi_j) = 0, \quad M(d\xi_i d\xi_j^*) = dt \delta_{ij}, \tag{3}$$

where  $M$  represents the ensemble average.

This unraveling of the master equation has many advantages. It is invariant under unitary transformations among the Lindblad operators, an invariance shared with the master equation, and which is unique to QSD. By taking the ensemble mean of the projector  $|\psi\rangle\langle\psi|$ , one reproduces the master equation above:  $M(|\psi\rangle\langle\psi|) = \rho$ . This gives a very simple interpretation for the relationship between the trajectories  $|\psi(t)\rangle$  and the density operator  $\rho$ :  $\rho(t)$  is the ensemble of all possible states  $|\psi(t)\rangle$ ; over the course of many runs of an experiment, the  $|\psi\rangle$ 's will tend to reproduce the density operator  $\rho$ , while in a single run, the system is in a state  $|\psi\rangle$  (which depends on the choice of unraveling). Thus, expectation values  $\langle \hat{O} \rangle_\rho$  calculated with a density operator  $\rho$  would include both the quantum expectation value  $\langle \hat{O} \rangle_\psi$  and the ensemble mean over all the  $|\psi\rangle$ s.

Numerically there is often a large advantage in representing a system by a state rather than a density operator. If it requires  $N$  basis states ( $2N$  real numbers) to represent the wavefunction, the density operator will require  $N^2$  real numbers. Thus, even though many runs may be required to produce an accurate answer, the factor of order  $N$  saved on each individual run can still result in large savings of computer time and memory. This is particularly true if one takes advantage of QSD's localization properties [10].

## 2.2 Decoherent histories

An extremely promising interpretation of quantum mechanics is the decoherent (or consistent) histories formalism, developed by Griffiths, Omnès, and Gell-Mann and Hartle [4, 5, 6, 7, 8]. In this formalism, quantum systems are described by sets of possible histories  $\{\alpha\}$ . These histories ascribe certain definite values, or ranges of values, to selected variables at successive points in time. Along with the histories, there is a *decoherence functional*  $D[\alpha, \alpha']$  on pairs of histories. For a set of histories  $\{\alpha\}$  to consistently describe the quantum system, they must satisfy the *decoherence criterion*

$$D[\alpha, \alpha'] = \delta_{\alpha\alpha'} p_\alpha, \quad (4)$$

where  $p_\alpha$  is the probability for the history  $\alpha$  actually to occur. If the decoherence criterion is met, then these histories obey the usual classical probability sum rules; one can assert that one or another history actually occurred, without the kind of interference effects seen in the two-slit experiment. In the case of Schrödinger's cat, one history would include a live cat and another a dead cat, without reference to observers or measurements.

In standard non-relativistic quantum mechanics, the usual choice of histories consists of an exhaustive set of orthogonal projection operators  $\{\hat{\mathcal{P}}_{\alpha_i}^i(t_i)\}$  at each time of interest  $t_i$ .

$$\sum_{\alpha_i} \hat{\mathcal{P}}_{\alpha_i}^i(t_i) = \hat{1}, \quad \hat{\mathcal{P}}_{\alpha_i}^i(t_i) \hat{\mathcal{P}}_{\alpha'_i}^i(t_i) = \delta_{\alpha_i \alpha'_i} \hat{\mathcal{P}}_{\alpha_i}^i(t_i). \quad (5)$$

These projections represent different alternatives at the time  $t_i$ . A single history  $\alpha$  represents a choice of one  $\hat{\mathcal{P}}_{\alpha_i}^i(t_i)$  at each time  $t_i$ , represented by the string of projection choices  $\alpha_i$ .

The decoherence functional can be written

$$D[\alpha, \alpha'] = \text{Tr} \left\{ \hat{\mathcal{P}}_{\alpha_n}^n(t_n) \cdots \hat{\mathcal{P}}_{\alpha_1}^1(t_1) \rho \hat{\mathcal{P}}_{\alpha'_1}^1(t_1) \cdots \hat{\mathcal{P}}_{\alpha'_n}^n(t_n) \right\}, \quad (6)$$

and a set of histories must satisfy (4).

One might be tempted to choose as a set of histories the precise values of some complete set of variables at each point in time. For example, for a single particle one might have its histories be its different possible trajectories  $x(t)$ . Histories of this sort almost never decohere. In general, a fair degree of *coarse-graining* is required to even approximately satisfy (4). Since finding exactly decoherent sets of histories is difficult, the usual course is to find a set of histories which satisfies the decoherence criterion to a finite level of accuracy [14]. It is conjectured that there is an exactly decoherent set of histories in a neighborhood of every such approximately decoherent set [15].

One simple (and therefore popular) type of coarse-graining is to separate the system into a distinguished subsystem and an environment [3, 8, 16]. Tracing over the environment then produces a set of coarse-grained histories in terms of the “distinguished variables” alone. It has been shown that under a wide variety of circumstances, histories coarse-grained in this way approximately decohere, with increasing precision as the distinguished system approaches the classical limit [3].

This type of coarse-graining brings us close to the situation of interest for quantum state diffusion. It has recently been shown that for a large class of open quantum systems there is a close connection between quantum state diffusion and decoherent histories [9]. The different possible QSD trajectories correspond to alternative histories; these histories approximately decohere, and occur with the same probabilities as in the decoherence formalism. In this context one can think of QSD as a dynamical form of the decoherent histories formalism, or decoherent histories as a global view of QSD.

### 3 Open quantum systems and the quasiclassical limit

### 3.1 Linear quantum systems

An important class of systems which can be treated with the QSD formalism are *linear systems*, with a Hamiltonian function quadratic in  $\hat{Q}$  and  $\hat{P}$ , and Lindblad operators given by a (not necessarily Hermitian) combination  $c_q\hat{Q} + c_p\hat{P}$ . These systems have been treated at length by a number of researchers [17, 18].

Halliwell and Zoupas [19] have shown that these linear systems tend to localize with time onto Gaussian wave packets in phase space. These wave packets follow paths in phase space which are close to paths defined by the classical (or quasiclassical) equations of motion.

From the QSD equation (2) the Itô equation for the expectation value of an observable is

$$\begin{aligned} d\langle\hat{O}\rangle &= \langle d\psi|\hat{O}|\psi\rangle + \langle\psi|\hat{O}|d\psi\rangle + \langle d\psi|\hat{O}|d\psi\rangle \\ &= -i\langle[\hat{O}, \hat{H}]\rangle dt + \langle\hat{L}^\dagger\hat{O}\hat{L} - \frac{1}{2}\{\hat{L}^\dagger\hat{L}, \hat{O}\}\rangle dt + (\langle\hat{O}\hat{L}\rangle - \langle\hat{O}\rangle\langle\hat{L}\rangle)d\xi + \\ &\quad (\langle\hat{O}\hat{L}^\dagger\rangle - \langle\hat{O}\rangle\langle\hat{L}^\dagger\rangle)d\xi^*. \end{aligned} \tag{7}$$

If the Hamiltonian is of the usual form

$$\hat{H} = \hat{P}^2/2m + V(\hat{Q}),$$

and the Lindblad operator  $\hat{L}$  is linear then we can readily evaluate this expression for simple operators  $\hat{O}$ .

Halliwell and Zoupas have shown that for linear systems one can, to a very good approximation, reduce the QSD equation to a set of coupled equations for  $\langle\hat{Q}\rangle$ ,  $\langle\hat{P}\rangle$ ,  $\langle\Delta\hat{Q}^2\rangle$ ,  $\langle\Delta\hat{P}^2\rangle$ , and  $\langle\Delta\hat{Q}\Delta\hat{P} + \Delta\hat{P}\Delta\hat{Q}\rangle$ . So long as the wave packet remains localized, so that the higher moments can be neglected, the QSD evolution can be reduced to these five equations. The equations for  $\langle\hat{Q}\rangle$  and  $\langle\hat{P}\rangle$  correspond to the equations of motion for a classical path in phase space, modified by the presence of noise and small diffusive corrections which depend on the higher moments.

This is similar to the Ehrenfest theorem for the Schrödinger equation, in which it can be shown that wave packets localized in phase space follow

approximately classical paths. Unlike the Ehrenfest theorem, however, in QSD this localization usually becomes better and better with time, rather than the reverse [13, 19].

## 3.2 Nonlinear quantum systems

While the equations of Halliwell and Zoupas were derived for linear systems, they provide a good approximation for the classical limit even of nonlinear systems. In this classical limit, the width of a localized wave packet is small compared to the spatial variance of the potential (and its higher derivatives). Thus, to the wave packet the potential seems locally quadratic, though slowly time-varying, and we would expect many of these localization results to apply.

In the classical limit, therefore, one can treat nonlinear problems by linearizing about the quasiclassical path, and solving for the moments of the wave packet. This is quite similar to the classical technique of linearizing about a known orbit to examine the behavior of nearby solutions.

Halliwell and Zoupas [19] have shown that solutions tend in the mean towards localized Gaussian wave packets when the third-derivative and higher terms in the potential are negligible, i.e., when

$$\langle V'(\hat{Q}) \rangle \approx V'(\langle \hat{Q} \rangle), \quad (8)$$

$$\langle \hat{Q} V'(\hat{Q}) \rangle - \langle \hat{Q} \rangle \langle V'(\hat{Q}) \rangle \approx \langle \Delta \hat{Q}^2 \rangle V''(\langle \hat{Q} \rangle), \quad (9)$$

and

$$\langle \hat{P} V'(\hat{Q}) + V'(\hat{Q}) \hat{P} \rangle - 2 \langle \hat{P} \rangle \langle V'(\hat{Q}) \rangle \approx \langle \Delta \hat{Q} \Delta \hat{P} + \Delta \hat{P} \Delta \hat{Q} \rangle V''(\langle \hat{Q} \rangle). \quad (10)$$

Numerical investigation [2, 10] as well as theoretical arguments [13] indicate that localization occurs in almost all systems, whether linear or not. If one thinks of QSD in terms of decoherence this is not surprising. Many people have shown that decoherence through interaction with an environment is extremely rapid. This corresponds to superpositions quickly reducing to highly localized states. In most cases, this localizing effect of the environment predominates over dispersive effects due to quantum spreading.

### 3.3 Localization and the moving basis

One practical consequence of localization is that it is possible, by choosing an appropriate basis, to reduce significantly the number of basis states needed to represent the wave packet [10]. If a wave packet is localized about a point  $(q, p)$  in phase space, it might require a great many of the usual number states  $|n\rangle$  to represent it. If instead we represent the wave packet in terms of *excited coherent states*  $|q, p, n\rangle = \hat{D}(q, p)|n\rangle$ , relatively few basis states are required, with obvious savings in terms of computer storage and computation time. Here,  $\hat{D}(q, p)$  is the coherent state displacement operator,

$$\hat{D}(q, p) = \exp \frac{i}{\hbar} (p\hat{Q} - q\hat{P}), \quad (11)$$

which displaces the excited state  $|n\rangle$  to the excited coherent state  $|q, p, n\rangle$  centered on  $(q, p)$ . This representation of the state by classical  $(q, p)$  and quantum  $|q, p, n\rangle$  is called the *moving basis* or *mixed* representation, or MQSD, and has been discussed extensively elsewhere [20, 10].

## 4 The Duffing oscillator

### 4.1 Quantizing the forced damped Duffing oscillator

A good example of a nonlinear system is the forced, damped Duffing oscillator. This has a classical equation of motion

$$\frac{d^2x}{dt^2} + 2\Gamma \frac{dx}{dt} + x^3 - x = g \cos(t), \quad (12)$$

and for some choices of  $\Gamma$  and  $g$  is chaotic [21].

Because the equation of motion includes explicit time-dependence, the solutions lie in a three-dimensional phase space  $x, p, t$ . It is helpful to consider a discrete surface of section of this system. Let  $(x_0, p_0)$  be the initial point of the forced, damped Duffing oscillator at time  $t_0 = 0$ . Then we

can define a *constant phase map* in the  $x$ - $p$  plane by the sequence of points  $(x_n, p_n) = (x(t_n), p(t_n))$  at times  $t_n = 2\pi n$ . Figure 1 illustrates this in the chaotic regime, where we can clearly see from the surface of section the fractal structure of the strange attractor.

Quantizing the Duffing oscillator is straightforward using the QSD formalism. The Hamiltonian operator is

$$\hat{H}(\hat{Q}, \hat{P}, t) = \hat{P}^2/2m + \hat{Q}^4/4 - \hat{Q}^2/2 + g \cos(t)\hat{Q} + \sqrt{\Gamma}(\hat{Q}\hat{P} + \hat{P}\hat{Q}), \quad (13)$$

and the damping is represented by a Lindblad operator

$$\hat{L} = 2\sqrt{\Gamma}\hat{a} = \sqrt{2\Gamma}(\hat{Q} + i\hat{P}), \quad (14)$$

where we have assumed  $\hbar = 1$ . The last term in the Hamiltonian is an ansatz, added to give the correct equations of motion in the classical limit; it is necessary due to the simplistic model of the dissipative environment.

This system is far from classical. To go to the classical limit, we introduce a scaling factor  $\beta$ ,

$$\hat{H}_\beta(\hat{Q}, \hat{P}, t) = \hat{P}^2/2m + \beta^2\hat{Q}^4/4 - \hat{Q}^2/2 + (g/\beta) \cos(t)\hat{Q} + \sqrt{\Gamma}(\hat{Q}\hat{P} + \hat{P}\hat{Q}). \quad (15)$$

As we reduce  $\beta$ , the scale of the problem (compared to  $\hbar$ ) increases by  $1/\beta$  in  $x$  and  $p$ , without altering the classical dynamics. Thus,  $\beta \rightarrow 0$  is the classical limit of this system. Classical behavior should emerge from the system in this limit. This is supported by the numerical calculations. (See section 4.3.)

## 4.2 Application to decoherent histories

The forced, damped Duffing oscillator has been treated elsewhere using the decoherent histories formalism [22, 23, 24]. While this approach has great theoretical power, it does not lend itself readily to numerical solution, which is generally necessary for this kind of nonlinear problem. Fortunately, as it has been shown that QSD is very closely related to a certain kind of coarse-grained decoherent history [9], one can use the numerically efficient QSD method to perform a quantum Monte Carlo calculation for open systems of this sort.

It has been argued [14, 8, 16, 22] that solutions of these open systems should peak about the quasiclassical equations of motion, i.e., they should behave in the classical limit like a classical problem with noise. This is amply demonstrated by the numerical results in section 4.3.

By choosing an appropriate set of decoherent histories one can find a quantum equivalent to the Poincaré surface of section defined by (12) above. Consider the times  $t_i = 2\pi i$ , with a set of projection operators  $\hat{\mathcal{P}}_{q_i, p_i}(t_i)$  onto local cells of phase space defined at each time, these cells centered at  $(q_i, p_i)$ . Although there are no true orthogonal projections onto cells of phase space, there are a number of approximate projections; the simplest are the coherent state projectors  $\hat{\mathcal{P}}_{qp} = |q, p\rangle\langle q, p|$ , and there are many others [5, 25, 26, 22, 27]. We can write down the decoherence functional

$$D[\{q_i, p_i\}, \{q'_i, p'_i\}] = \text{Tr} \left\{ \hat{\mathcal{P}}_{q_n, p_n}(t_n) \cdots \hat{\mathcal{P}}_{q_1, p_1}(t_1) \rho \hat{\mathcal{P}}_{q'_1, p'_1}(t_1) \cdots \hat{\mathcal{P}}_{q'_n, p'_n}(t_n) \right\}, \quad (16)$$

where  $\rho = |\psi\rangle\langle\psi|$  is the initial density operator, for simplicity taken to be pure.

It has been shown that in systems which interact strongly with an environment, the off-diagonal terms of the decoherence functional decay very rapidly. So long as the time between projections  $t_{i+1} - t_i$  is large compared to the decoherence time  $t_D$ , and the phase space cells are large compared to  $\hbar$ , the histories described by (16) will decohere to a good level of precision. In the quasiclassical limit, the probabilities  $D[\{q_i, p_i\}, \{q_i, p_i\}]$  should be sharply peaked about the classical solution.

As shown by Diósi, Gisin, Halliwell and Percival [9], quantum state diffusion trajectories will give the same probabilities as the decoherence functional for histories which project onto the same quantities (in this case coherent states in phase space) and are at least as coarse-grained as the level of QSD localization. By following a QSD trajectory, therefore, and looking at the expectation values of  $\langle\hat{Q}\rangle$  and  $\langle\hat{P}\rangle$  at the times  $t_i$ , one has picked out a single decoherent history with the correct probability.

### 4.3 Numerical example

We solved the forced, damped Duffing oscillator numerically by integrating the QSD equation, both in full (using MQSD) and in the linearized approximation of Halliwell and Zoupas, using a C++ quantum simulation package we have developed [10, 28]. All of these results were generated on standard 486 PC's running LINUX.

The classical unscaled problem is bounded within a small region of phase space. (See figure 1.) Clearly, the quantized version of this problem (with  $\hbar = 1$ ) should be far from the classical limit. One would expect to observe little trace of the classical fractal structure. The expectation values of  $\hat{Q}$  and  $\hat{P}$  should be dominated by noise.

Examining figure 2a, we see that the results of the numerical calculation match our expectations very well. The expectation values appear randomly distributed; they are dominated almost completely by the stochastic terms of the equation.

Approaching the classical limit  $\beta \rightarrow 0$ , more and more of the classical structure of the attractor appears. At first the broad outlines of the attractor are formed, then increasing levels of substructure. (Figures 2b–2d.) The full fractal structure of a strange attractor is only attainable in an unphysical purely classical limit. In an actual physical system, the uncertainty principle provides a lower cutoff to the scale-invariance of the strange attractor. It is unphysical to discuss regions of phase space with areas smaller than Planck's constant.

In fact, the actual lower cutoff is even larger than that, due to the interaction with the environment. Classically, one can eliminate noise from the environment by going to the limit of zero temperature. In quantum systems, though, there is noise even in this limit – the equivalent of zero point noise for the degrees of freedom of the reservoir. The existence of this noise is closely related to the fact that in general, coarse-grainings much coarser than would be naïvely suggested by the uncertainty principle are required for decoherence [22]; in general, phase space cells large compared to  $\hbar$  are required.

## 4.4 The linearized theory

The linearized equations are expected to remain valid as long as the potential is approximately locally quadratic, i.e., as  $\beta \rightarrow 0$ . This approximation takes advantage of QSD's unique localization properties. We can solve these equations, suitably modified by the presence of the ansatz in (15), for different values of  $\beta$ , and compare them to results generated with the full QSD code. The results are displayed in figures 3a–3d.

We see that at  $\beta = 1$  the linearized equations are completely wrong (figure 3a). As we reduce  $\beta$ , however, the two methods come into better and better agreement, until at  $\beta = 0.01$  the agreement is nearly perfect (figures 3b–3d).

The linearized equations are thus only valid when one goes very far toward the quasiclassical limit. In this regime, however, the computational advantage over the full equations is enormous; for  $\beta = 0.01$  it is  $10^4$ . In the intermediate regime of  $\beta \sim 0.1$ , the linearized approximation is no longer valid, but localization can still provide a tremendous advantage. Using the MQSD algorithm, one can represent the system by 10–20 basis states, as opposed to the  $\sim 1000$  basis states which would be needed by QSD without the moving basis algorithm and more than  $10^6$  real numbers which would be required to solve the master equation.

## 5 Conclusions

Many criteria have been suggested to define chaos in quantum systems. These differ in their emphasis and domain of application. But nearly all are based on the premise that, as one approaches the classical realm, quantum systems should behave more and more like classical chaotic systems. This limit is difficult in the closed systems which are usually studied. By contrast, for open systems the classical limit arises naturally.

Quantum state diffusion provides a vivid picture of how this crossover from quantum to classical occurs. As a quantum system becomes macroscopic, it increasingly resembles a localized wave packet, following an approximately

classical path in phase space. At short length scales, its evolution is dominated by quantum mechanical uncertainties, due to quantum spreading and the random influence of the environment. As one approaches the classical limit, these stochastic influences become less important, being replaced by the uncertainties of classical chaos.

This is clearly illustrated by the numerical results of QSD simulations. These demonstrate the value of QSD as a practical algorithm for solving the master equation. By making use of QSD's unique localization properties, the equations can be solved numerically with far greater efficiency than would be possible in solving the master equation directly [10].

Going to the classical limit this advantage is even more pronounced; one may replace the full QSD equations by a linearized approximation, requiring the solution of only 5 coupled ordinary differential equations [19]. This approximation provides not only a powerful numerical tool, but also demonstrates how quasiclassical equations of motion rise from the underlying quantum theory.

QSD also provides a practical method of calculating results in the decoherent histories formalism of quantum mechanics. While decoherent histories provides a powerful interpretive tool, it does not necessarily lend itself to practical calculations; it is often difficult to solve for the probabilities of individual histories. For open systems, QSD generates such histories automatically, with their correct probabilities. The arguments of Gell-Mann and Hartle, that probabilities will peak about quasiclassical histories in the classical limit, are supported by the QSD analysis of this limit, and by the numerical results presented in this paper.

## Acknowledgments

We thank the EPSRC in the UK for financial support, and gratefully acknowledge M Gell-Mann, N Gisin, J Halliwell, J Hartle, S Lloyd, J Paz, J Ralph, M Rigo, T Spiller, W Strunz, and W Zurek for many valuable communications. TAB performed some of this work while visiting the University

of Geneva.

## References

- [1] E. Joos and H.D. Zeh, *Z. Phys. B* **59**, 223 (1985).
- [2] N. Gisin and I.C. Percival, *J. Phys. A* **25**, 5677 (1992). *J. Phys. A* **26**, 2233 (1993). *J. Phys. A* **26**, 2245 (1993).
- [3] W. Zurek, *Phys. Rev. D* **24**, 1516 (1981). W. Zurek, *Phys. Rev. D* **26**, 1862 (1982).
- [4] R. Griffiths, *J. Stat. Phys.* **36**, 219 (1984). “A Consistent History Approach to the Logic of Quantum Mechanics,” to appear in the proceedings of the Symposium on the Foundations of Modern Physics, Helsinki, Finland (1994). “Consistent Quantum Reasoning,” CMU preprint (1995).
- [5] R. Omnès, *J. Stat. Phys.* **53**, 893 (1988). *J. Stat. Phys.* **53**, 933 (1988). *J. Stat. Phys.* **53**, 957 (1988). *J. Stat. Phys.* **57**, 357 (1989). *Rev. Mod. Phys.* **64**, 339 (1992). *The Interpretation of Quantum Mechanics*, Princeton University Press, Princeton (1994).
- [6] M. Gell-Mann and J. Hartle, in *Complexity, Entropy, and the Physics of Information*, SFI Studies in the Sciences of Complexity v.8, ed. by W. Zurek, Addison-Wesley, Reading (1990).
- [7] M. Gell-Mann and J. Hartle, Proceedings of the 25th International Conference on High-Energy Physics, Singapore, 1303 (1990).
- [8] M. Gell-Mann and J. Hartle, *Phys. Rev. D* **47**, 3345 (1993).
- [9] L. Diósi, N. Gisin, J. Halliwell and I.C. Percival, *Phys. Rev. Lett.* **74**, 203 (1995).
- [10] R. Schack, T.A. Brun and I.C. Percival, *J. Phys. A*, **28**, 5401 (1995).
- [11] T.P. Spiller and J.F. Ralph, *Phys. Lett. A*, **194**, 235 (1994).
- [12] G. Lindblad, *Commun. Math. Phys.* **48**, 119 (1976).
- [13] I.C. Percival, *J. Phys. A* **27**, 1003 (1994).

- [14] F. Dowker and J.J. Halliwell, Phys. Rev. D **46**, 1580 (1992).
- [15] F. Dowker and A. Kent, submitted to J. Stat. Phys. (1995).
- [16] T. Brun, Phys. Rev. D **47**, 3383 (1993).
- [17] L. Diósi, Phys. Lett. A, **129**, 419 (1988).
- [18] Y. Salama and N. Gisin, Phys. Lett. A, **181**, 269 (1993).
- [19] J. Halliwell and A. Zoupas, “Quantum State Diffusion, Density Matrix Diagonalization and Decoherent Histories: A Model,” to appear Phys. Rev. D (1995).
- [20] T. Steimle, G. Alber and I.C. Percival, J. Phys. A, **28**, L491 (1995).
- [21] M.C. Gutzwiller, *Chaos in Classical and Quantum Mechanics*, Springer-Verlag New York (1990). J. Guckenheimer and P. Holmes, *Nonlinear Oscillations, Dynamical Systems, and Bifurcations of Vector Fields*, Springer-Verlag New York (1983).
- [22] T. Brun, *Applications of the Decoherence Formalism*, Caltech Ph.D. thesis (1994).
- [23] T. Brun, “Quantum Dissipative Chaos,” Caltech preprint CALT-68-1882 (1993).
- [24] T. Brun, Phys. Lett. A, **207**, 167 (1995).
- [25] J.J. Halliwell, Phys. Rev. D **46**, 1610 (1992).
- [26] J. Twamley, Phys. Rev. D **45**, 5730 (1993).
- [27] C. Anastopoulos, “Decoherence and classical predictability of phase space histories,” Imperial College preprint (1995).
- [28] R. Schack and T.A. Brun, in preparation.

Figure 1. The constant phase surface of section for the classical forced, damped Duffing oscillator in the chaotic regime,  $\Gamma = 0.125$ ,  $g = 0.3$ .

Figure 2. The constant phase surface of section for a single QSD trajectory of the quantum forced, damped Duffing oscillator in the chaotic regime,  $\Gamma = 0.125$ ,  $g = 0.3$ , for four scalings: a)  $\beta = 1.0$ , b)  $\beta = 0.25$ , c)  $\beta = 0.1$ , d)  $\beta = 0.01$ .

Figure 3. The constant phase surface of section for a single linearized QSD trajectory of the quantum forced, damped Duffing oscillator in the chaotic regime,  $\Gamma = 0.125$ ,  $g = 0.3$ , for four scalings: a)  $\beta = 1.0$ , b)  $\beta = 0.25$ , c)  $\beta = 0.1$ , d)  $\beta = 0.01$ .

Figure 1. The classical Duffing oscillator surface of section.

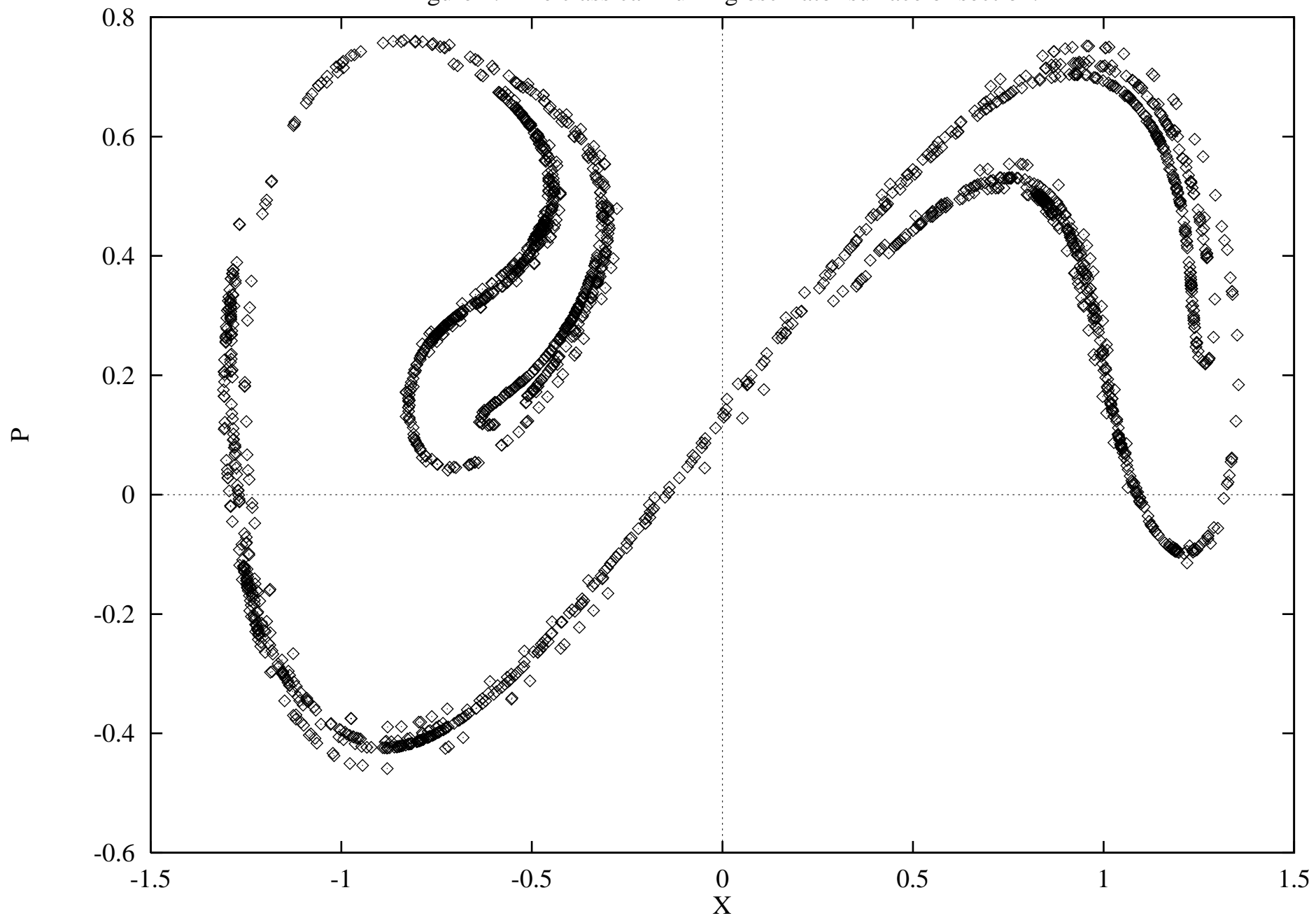


Figure 2a. QSD solution.

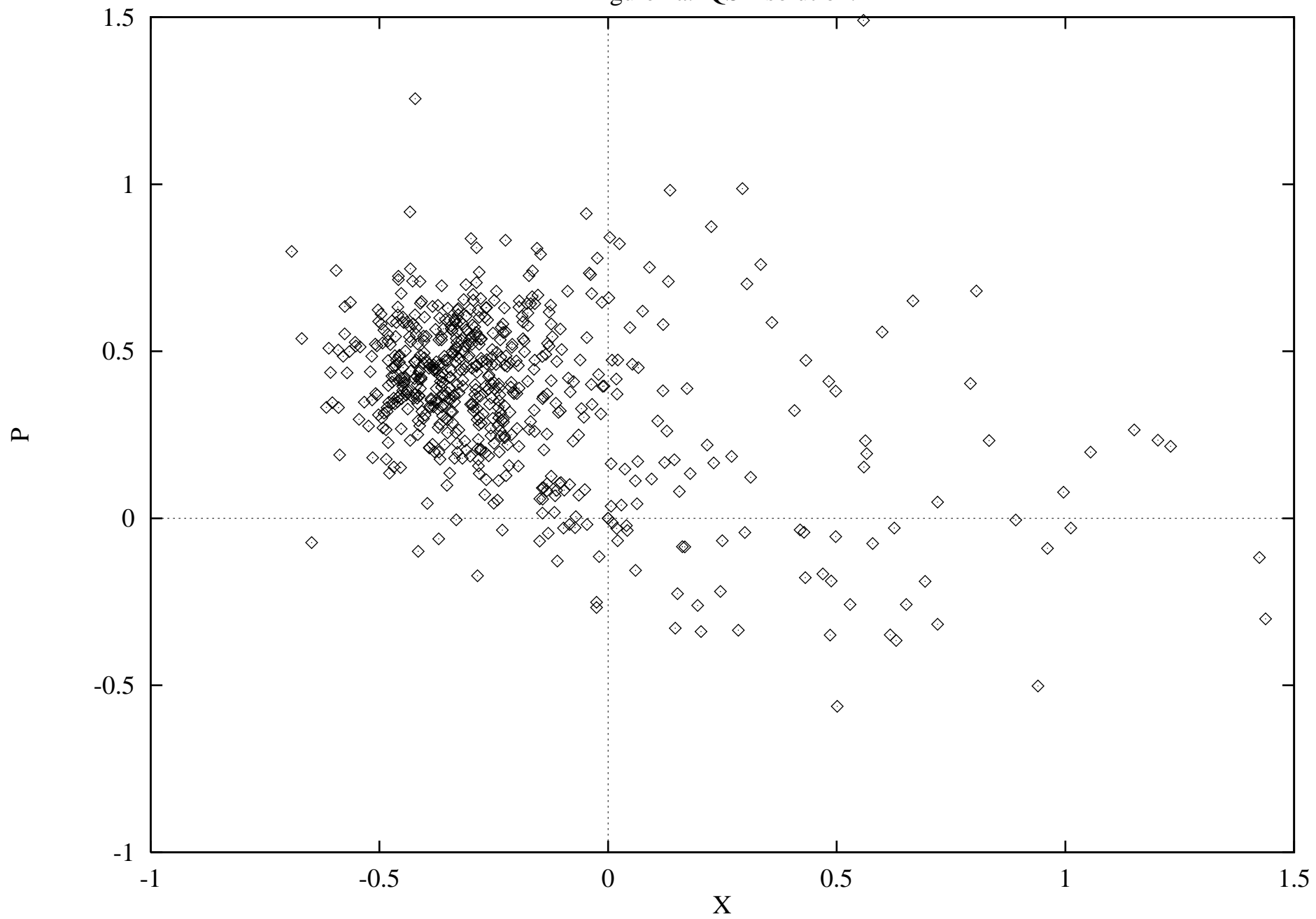


Figure 2b. QSD solution.

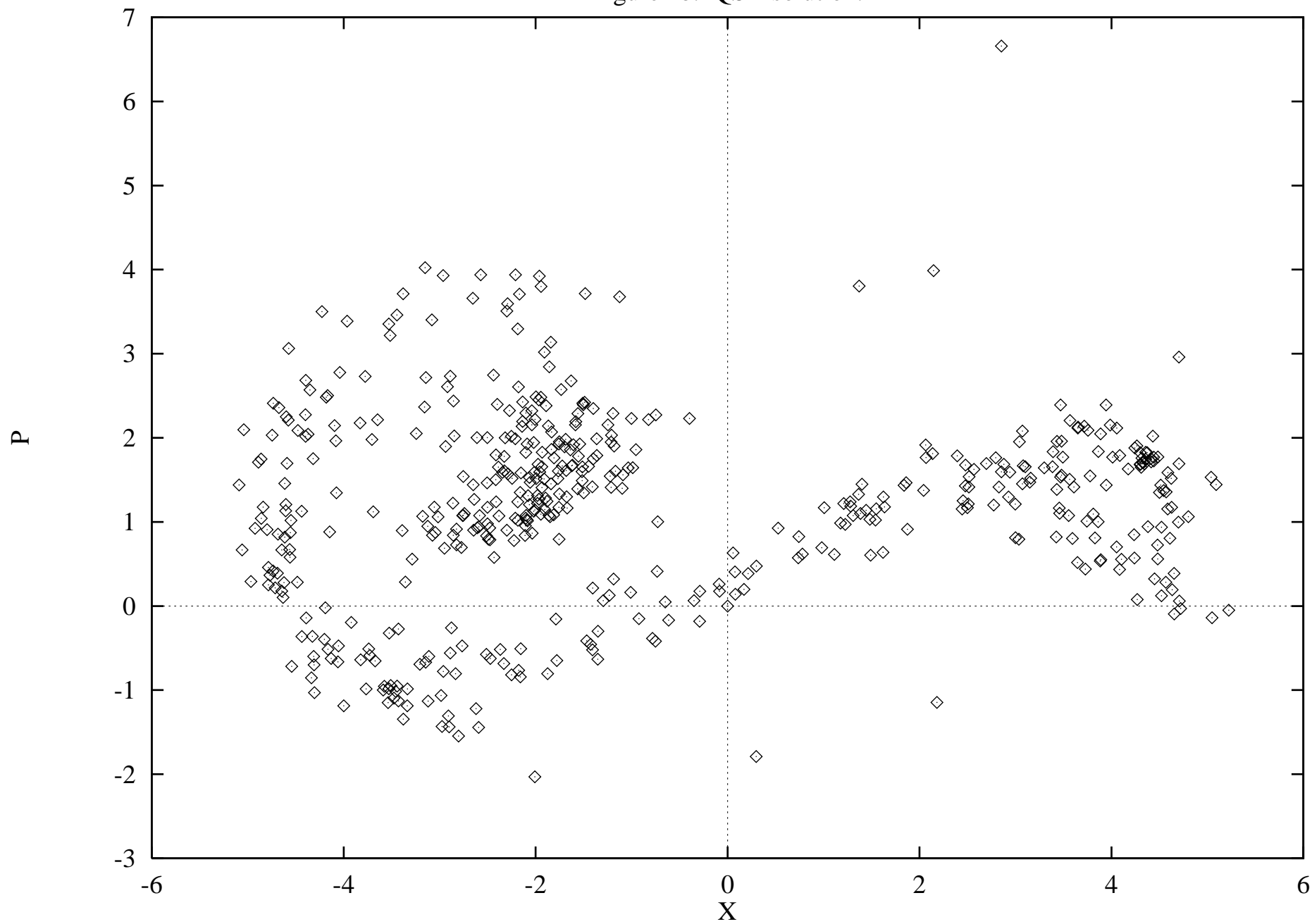


Figure 2c. QSD solution.

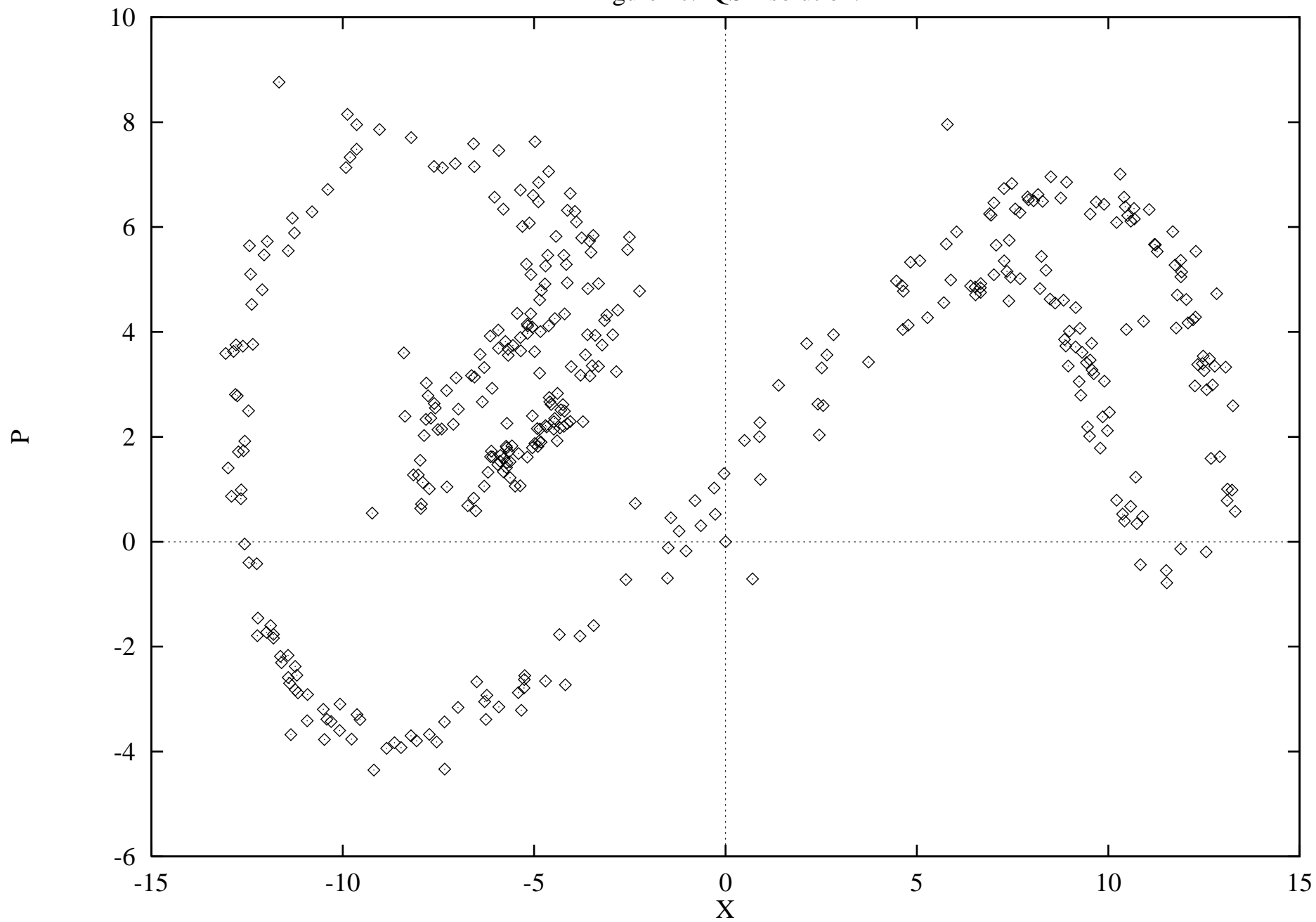


Figure 2d. QSD solution.

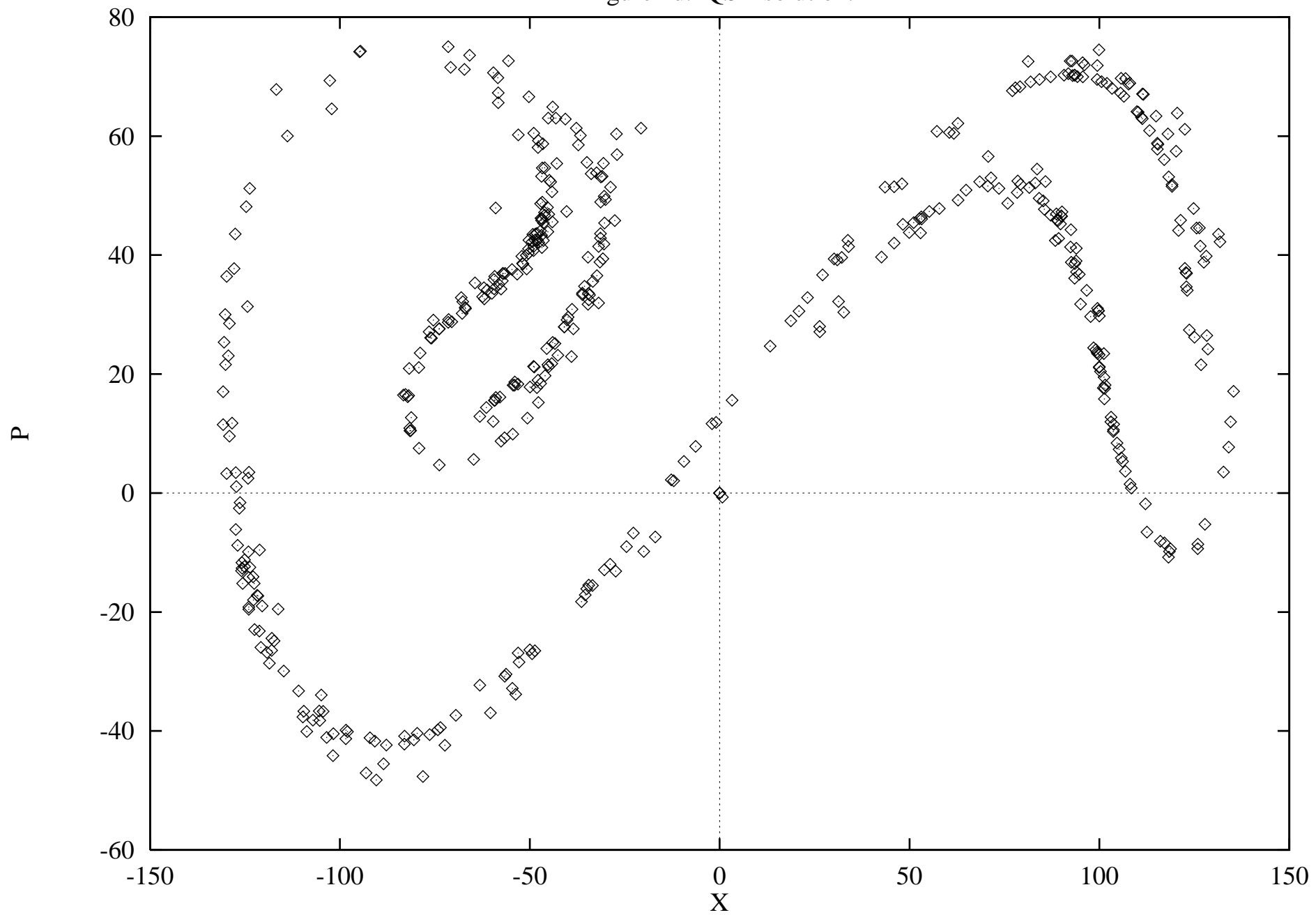


Figure 3a. Linearized QSD solution.

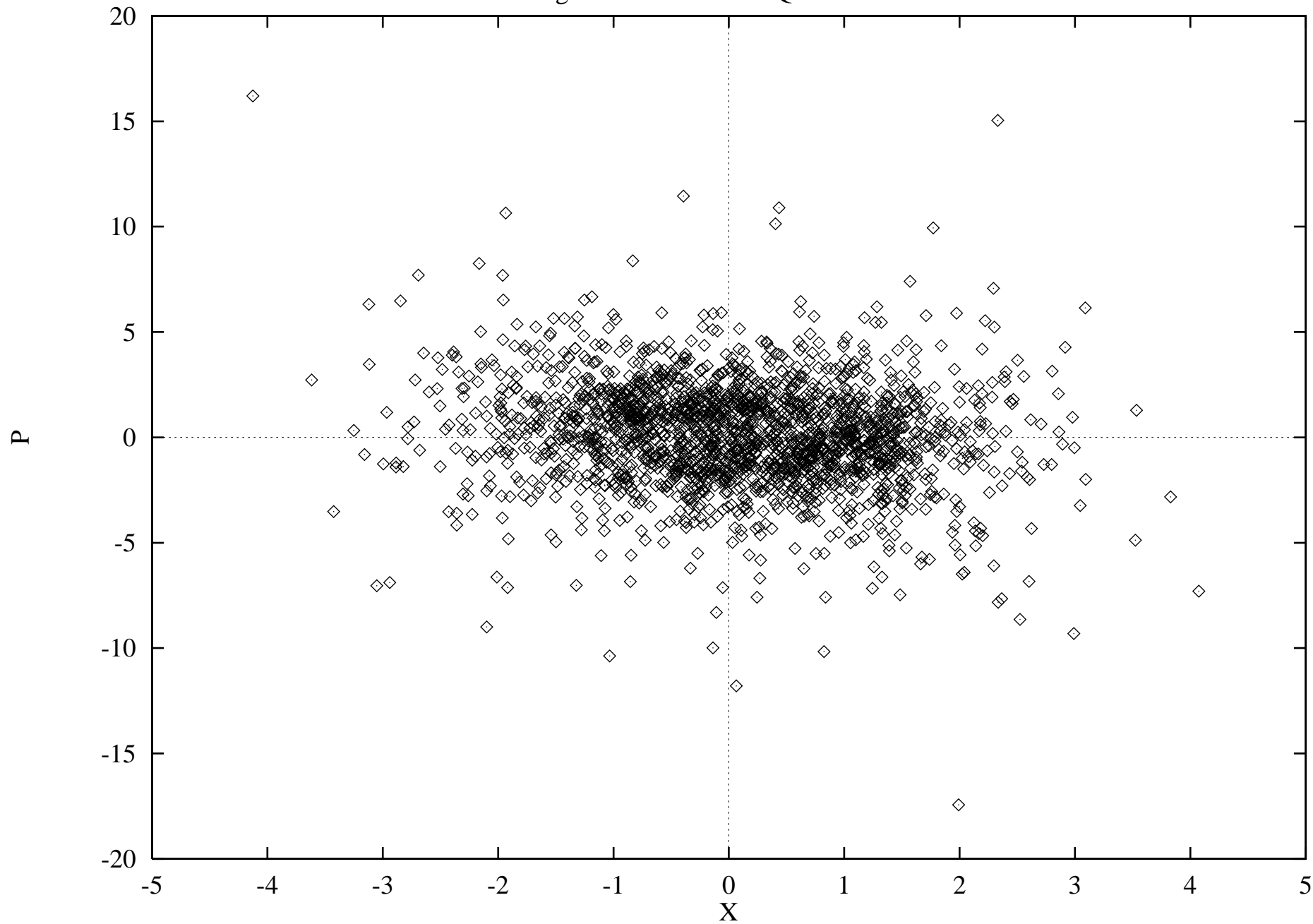


Figure 3b. Linearized QSD solution.

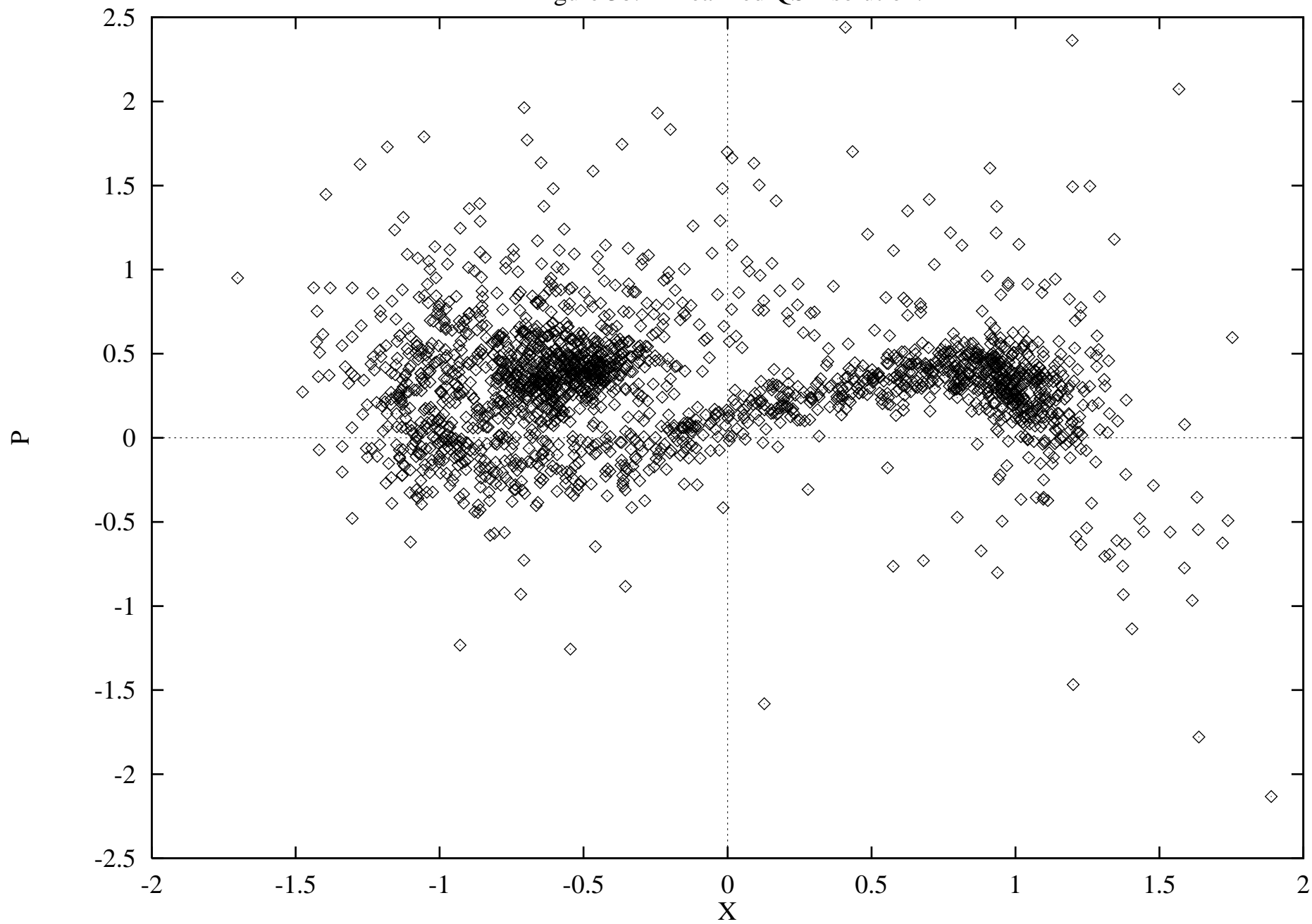


Figure 3c. Linearized QSD solution.

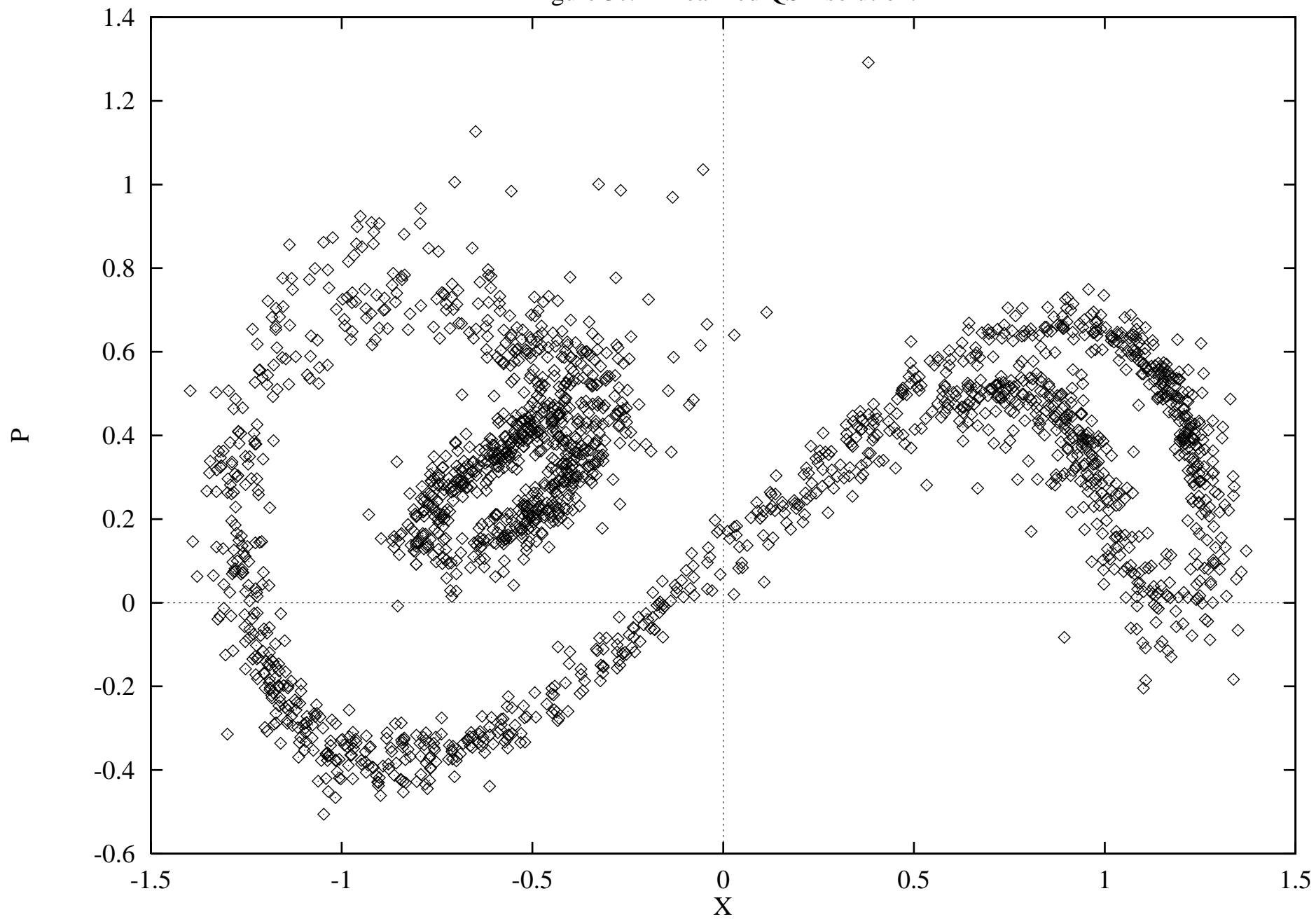


Figure 3d. Linearized QSD solution.

